

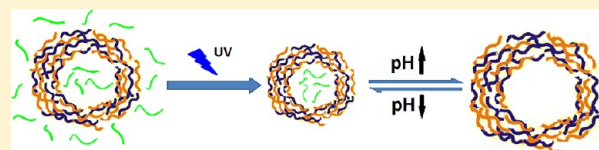
# UV-Cross-Linkable Multilayer Microcapsules Made of Weak Polyelectrolytes

Qiangying Yi, Dongsheng Wen, and Gleb B. Sukhorukov\*

School of Engineering and Materials Science, Queen Mary, University of London

**S** Supporting Information

**ABSTRACT:** Microcapsules composed of weak polyelectrolytes modified with UV-responsive benzophenone (BP) groups were fabricated by the layer-by-layer (LbL) technique. Being exposed to UV lights, capsules shrunk in the time course of minutes at irradiation intensity of 5 mW/cm<sup>2</sup>. The shrinkage adjusted the capsule permeability, providing a novel way to encapsulate fluorescence-labeled dextran molecules without heating. Cross-linking within the capsule shells based on hydrogen abstraction via excited benzophenone units by UV showed a reliable and swift approach to tighten and stabilize the capsule shell without losing the pH-responsive properties of the weak polyelectrolyte multilayers.



## INTRODUCTION

Stimuli-responsive vesicles possessing different functionalities are widely used as delivery systems in various fields ranging from medicine, pharmaceuticals, and chemical synthesis to catalytic applications.<sup>1</sup> In particular, light-addressable vesicles have received intensive interest recently, as their micro/nanostructures can be tuned remotely by lights (e.g., sunlight) without involving direct contact or interaction. The development of highly light-sensitive vesicles is of great importance in the fields of surface science and environmental applications, where sometimes light would be the only available stimulus to drive the systems. Various strategies were applied to develop light-addressable vesicles with different functionalities. For applications in agriculture and cosmetics, UV–Vis sensitive vesicles are the optimized options due to the abundance of sunlight. Meanwhile, Near-IR (NIR) absorbing vesicles are of greater interest in turbid media (e.g., biological tissues or pharmaceutical solids) because of the deep penetration and low light scattering at specific wavelengths. For example, chromophores, either photoreactive<sup>2</sup> or photocleavable,<sup>3</sup> in microcontainer systems could improve size shrinkage, adjust shell permeability, and modulate the release of encapsulated materials in the presence of NIR. Light-induced heating provides an alternative way for controlled release of the encapsulated materials by incorporating metal and metal oxide nanoparticles such as Au,<sup>4</sup> Ag,<sup>5</sup> and Fe<sub>3</sub>O<sub>4</sub>.<sup>6</sup>

Light-addressable vesicles demonstrate a novel channel to activate material delivery remotely, with emphasis on either encapsulation or release. However, the development of an intelligent or smart delivery system would be more complicated in practice, where more complex functionalities or multifunctionalities are required to satisfy different external stimulus triggers (i.e., enzymes, temperature, pH, ionic strength<sup>1c</sup>). Therefore, the integration of two or more stimuli-responsive functionalities in one vesicle system has important implications. As a practical matter, layer-by-layer (LbL) assembly would be a

promising technique to achieve the goals due to its simplicity and versatility.<sup>7</sup> By using the electrostatic interactions between oppositely charged polyelectrolytes, LbL capsules could be made with tunable size, composition, and stability,<sup>8</sup> endowing the capsules with unique properties for particular applications.<sup>9</sup> In addition, the step-by-step polymer deposition of the multilayers facilitates the modification of the fabricated capsules, providing opportunities to engineering a novel class of capsules with desired structures, chemical groups, and reactive functional sites. Furthermore, if the multilayer shells are composed of weak polyelectrolytes, the resulting capsules will automatically have a pH-responsive property. Consequently, LbL assembly offers a relatively simple and effective way to introduce a pH-responsive property at the very beginning of the capsule fabrication. In return, the pH-responsive property allows the control of the shrink–swell behaviors of capsule shell reversibly as a consequence of the dissociation equilibrium of the weak polyelectrolyte complex. Thus, a controlled release could be achieved through the controllable shell thickness or permeability, as well as the deconstruction of the capsule by adjusting the acidity of the surrounding solution.

In this work, we are aiming at fabricating the multilayer capsules with UV light induced changes and exploring their possible applications. It has been shown that, by responding to a certain UV wavelength, capsules are able to alter shell thickness, permeability, and multilayer arrangement.<sup>2</sup> Specifically, chemically stable benzophenone (BP) is widely used as a photoactivatable reagent to functionalize or reconstruct the remote C–H bonds in flexible molecular chains.<sup>10</sup> The highly efficient and good site-specific covalent modifications of macromolecules make BP a promising candidate for capsule

**Received:** March 8, 2012

**Revised:** June 19, 2012

**Published:** June 25, 2012

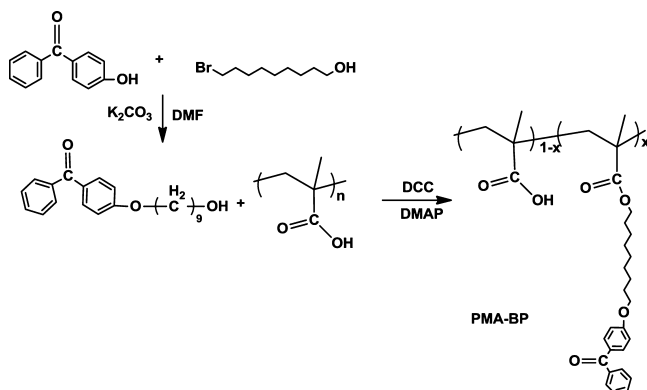
modification. Upon irradiation at a certain wavelength, BPs react with unreactive C–H bonds predominately. The introduction of BP groups in the multilayers will therefore endow the LbL capsules with novel UV responsive properties. In addition, microcapsules or multilayers composed of weak polyelectrolytes are sensitive to outer pH stimuli. It is possible to adjust reversibly the fabricated capsule's shrink–swell behavior by altering the environmental pH values.<sup>11</sup> Here, we reported the fabrication and characterization of microcapsules composed of weak polyelectrolytes with UV-absorbable BP groups. With these BP groups, the chemical and physical properties of polyelectrolyte capsules could be controlled and altered remotely, while preserving the pH-responsive properties of the weak polyelectrolyte multilayers. Furthermore, the envisaged potential applications of those capsules upon direct exposure to UV light and various pH environments were examined.

## MATERIALS AND METHODS

Poly(methacrylic acid) (PMA, MW = 100 kDa) was purchased from Polysciences Inc. Poly(allylamine hydrochloride) (PAH,  $M_w$  = 70 kDa), 4-hydroxybenzophenone, 9-bromo-1-nonanol,  $N,N'$ -dicyclohexylcarbodiimide, 4-(dimethylamino) pyridine, and other chemicals were purchased from Sigma-Aldrich. All chemicals were used as received without further purification.

**Synthesis of Benzophenone-Substituted Poly(methacrylic acid) (PMA-BP).** First, 4-(9-hydroxynonyloxy)benzophenone was synthesized in the same way as previously reported.<sup>12</sup> Then, benzophenone-substituted poly(methacrylic acid) was synthesized as in Scheme 1. Briefly, PMA (2.0446 g, 23.75 mmol) was dispersed in 30

**Scheme 1. Synthetic Scheme of Benzophenone-Substituted Poly(methacrylic acid), PMA-BP**



mL Dimethyl sulfoxide (DMSO), 4-(dimethyl-amino) pyridine (DMAP, 1 mmol), and 4-(9-hydroxynonyloxy)benzophenone (2.5 mmol) were added at 0 °C. The mixture was then stirred for 1 h, and  $N,N'$ -dicyclohexyl carbodiimide (DCC, 2.5 mmol) was added three times at 30 min intervals. After 6 h, the reaction was left overnight and the solution temperature was increased to room temperature gradually. After the reaction, the insoluble substance was filtered and the filtrate was concentrated under vacuum. The filtrate was reprecipitated in a large amount of acetone and dried under vacuum. The degree of substitution of the benzophenone group was estimated at ~50%, calculated from  $^1H$  NMR ( $D_2O$ , 600 MHz, Bruker) (as shown in Supporting Information Figure S1):  $\delta$  (ppm) 1.13–1.15 (t,  $-CH_3$ ), 2.19 (s,  $-CH_2-$ ), 3.59–3.63 (m,  $O=C-O-CH_2-$ ,  $-CH_2-O-BP$ ), 2.78–3.01 (m,  $-(CH_2)_6-$ ), 4.68 (s,  $H_2O$ ), 7.82–7.99 (m, H of BP group).

**Capsule Preparation.** Multilayers were assembled on the templates by the layer-by-layer technique as described previously.<sup>13</sup> Prior to the assembly,  $SiO_2$  particles ( $4.99 \pm 0.22 \mu m$ , Microparticles GmbH) were first treated with a solution of 25%  $NH_3$ /30%  $H_2O_2$ /

$H_2O$  (1:1:5) for 15 min at 75 °C to ensure a better attachment of the first polymer layer to the  $SiO_2$  surface,<sup>14a</sup> and then washed 3 times with pure water (resistivity 18.2  $M\Omega/cm$ ). PMA-BP solution (2 mg/mL in a mixture of 1:1 methanol and  $H_2O$ , 0.5 M NaCl) was adjusted to pH = 6. Polyelectrolytes were deposited on the  $SiO_2$  templates alternately for 15 min, starting with the positively charged PAH (2 mg/mL in 0.5 M NaCl), followed by three wash steps. To avoid aggregation, polymer-coated particles were ultrasonicated 10 s after every wash step. After the polymer deposition steps, the  $SiO_2$  templates were dissolved with a 0.2 M  $NH_4F$  and HF buffer solution at pH = 4.5.<sup>15</sup> (PAH/PMA-BP)<sub>4</sub> hollow capsules were obtained after several wash steps. Capsules (PAH/PMA)<sub>4</sub> without the BP groups and capsules (PAH/PSS)<sub>4</sub> without poly(methacrylic acid) polymer chains were also prepared and investigated in the following experiments as controls.

**Film Preparation.** Quartz slides were carefully cleaned in the same way as  $SiO_2$  particles in the procedure mentioned above. Layer-by-layer deposition was carried out by hand. The slides were alternately immersed in oppositely charged PAH and PMA-BP solution for 8 min each, followed by a 3 min wash.

**UV Irradiation.** UV irradiation was provided by a mercury lamp (UVACUBE 100, Honle UV Technology) ranging from 200 to 600 nm. The hollow capsules were dispersed in pure water in a cuvette, and exposed to UV light directly. The power used to irradiate the samples was measured to be approximately 5 mW/cm<sup>2</sup>. The dispersions were continuously stirred with a magnetic stirrer during UV irradiation. To reduce the bulk temperature increase during UV-irradiation, an ice bath was applied to ensure that the temperature change of the capsule suspension is less than 5 °C.

**Scanning Electron Microscopy (SEM) and Transmission Electron Microscopy (TEM).** Morphology changes of the (PAH/PMA-BP)<sub>4</sub> hollow capsules before and after UV irradiation were observed by SEM and TEM. Capsule suspension was dropped on a glass wafer, air-dried, and coated with gold before SEM observation (Hitachi S570). For TEM measurements, a high-resolution TEM (JEOL 2010) operating at 200 kV was used. Capsule suspension was deposited on a carbon-coated copper grid, and air-dried for several hours.

**Atomic Force Microscopy (AFM).** The thickness of the capsules was determined by an AFM system (Ntegra Therma, NT-MDT, Russia), where a drop of the capsule suspension was placed onto a silicon wafer and air-dried at room temperature. The single-shell thickness of a capsule was then estimated as the half-height of the flat region of a dried collapsed capsule.

**UV–Vis Spectroscopy.** A UV–Vis spectrophotometer (LAMBDA 950, Perkin-Elmer) was employed to investigate the UV absorption of the polyelectrolytes and LbL multilayer films. Aqueous solution measurements were made by using quartz cuvettes. LbL multilayer film spectra were obtained from samples deposited on quartz slides.

**Fourier Transform Infrared (FTIR).** FTIR spectra of vacuum-dried capsule samples with and without irradiation were obtained using infrared spectroscopy (FTIR spectrometer 100, Perkin-Elmer). All data were collected at a spectral resolution of 4  $cm^{-1}$ .

**Capsule Permeability and Stability.** Capsule permeability and stability were investigated by confocal laser scanning microscopy (CLSM) measurement. Briefly, (PAH/PMA-BP)<sub>4</sub> capsules were mixed with AF488 labeled dextran solution (1 mg/mL, MW = 10 kDa, Invitrogen) for appropriately 1 h to ensure complete dye permeation of capsules. Then, the mixture was placed under the UV lamp for specified durations. After UV irradiation, capsule suspensions were centrifuged, washed three times with pure water, and observed with a Leica TS confocal scanning system (Leica, Germany) equipped with a 63 $\times$ /1.4 oil immersion objective. For the stability studies, the (PAH/PMA-BP)<sub>4</sub> capsules were visualized by the incorporation of a rhodamine-labeled polymer (PAH-TRITC)<sup>16</sup> during the capsule preparation, and the pH of capsule suspensions was carefully adjusted with 0.1 M HCl and 0.1 M NaOH. The diameter of the capsules was determined by the Image-Pro Plus v 6.0 software.

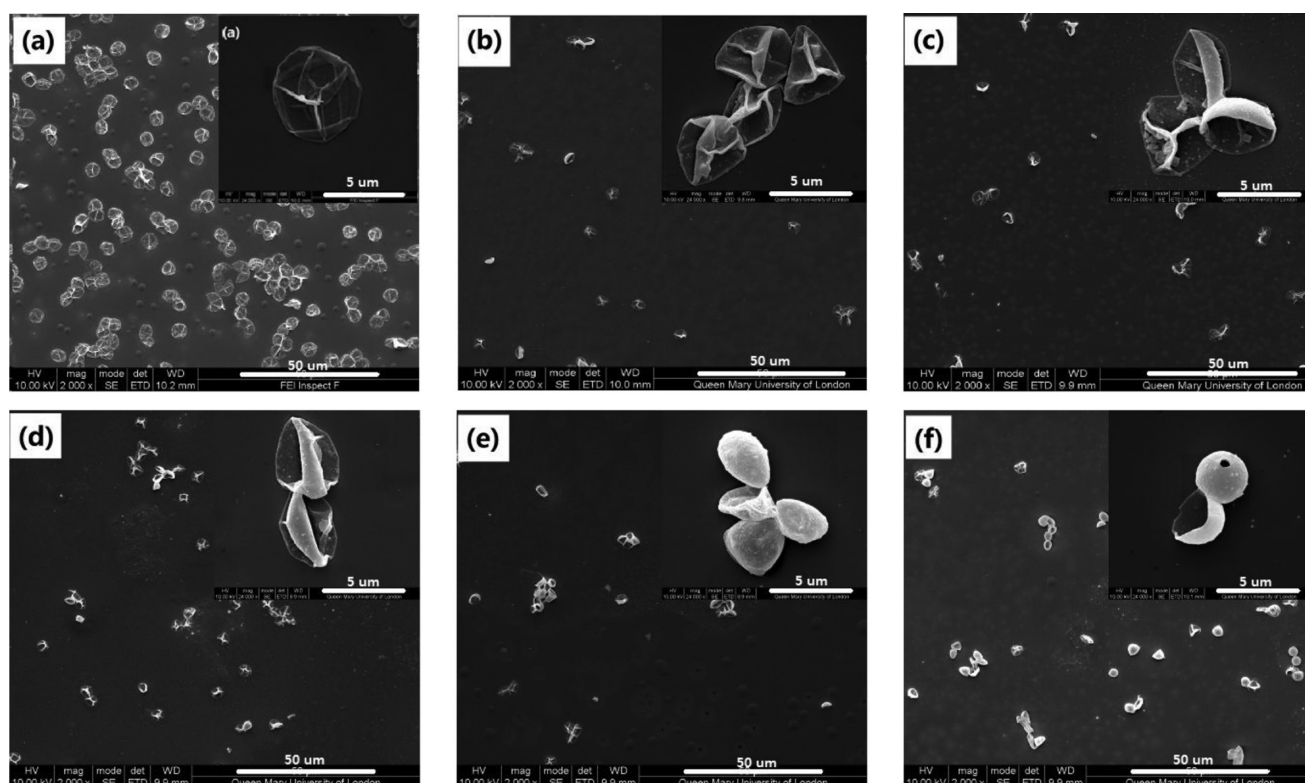


**Figure 1.** SEM images of  $(\text{PAH/PMA-BP})_4$  capsules before (a), and after UV irradiation for 15 (b), 30 (c), 60 (d), 90 (e), and 120 min (f).

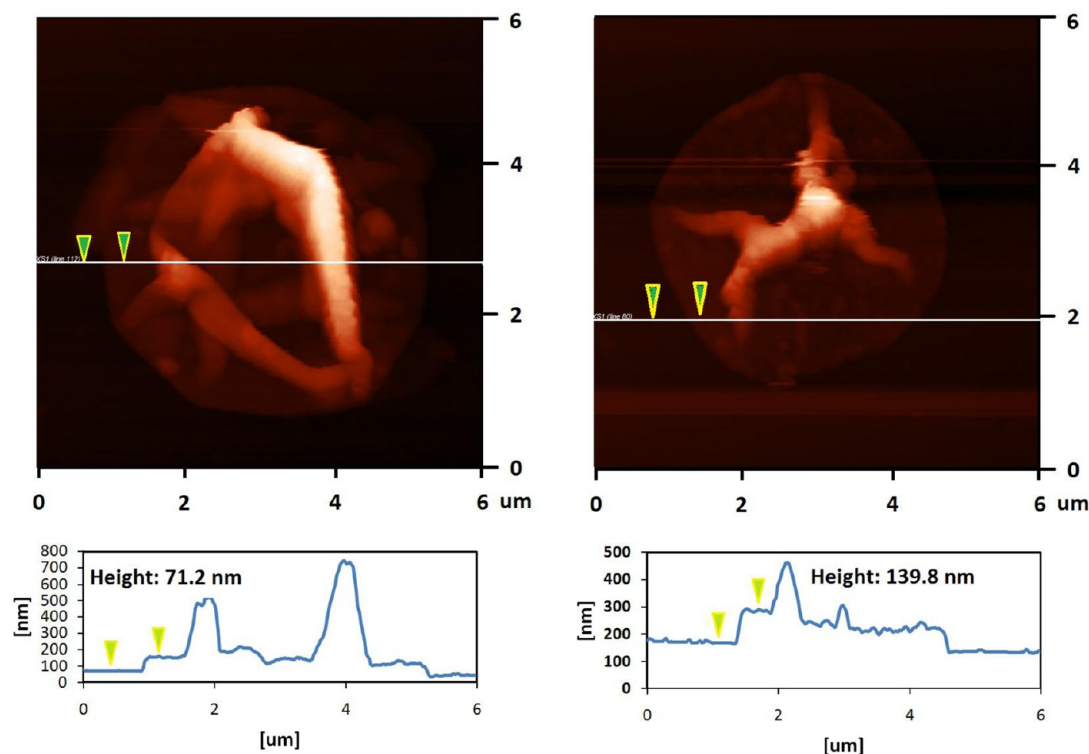


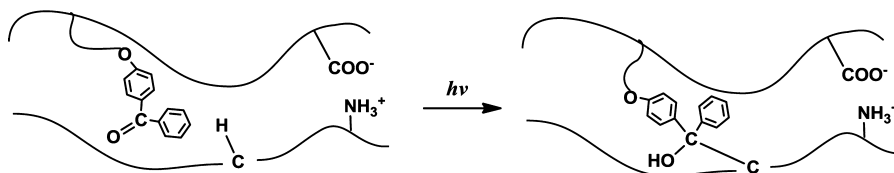
**Figure 2.** AFM images (top) and cross-section profiles (bottom) of  $(\text{PAH/PMA-BP})_4$  capsules before (left) and after (right) UV irradiation for 120 min. The height (single shell thickness  $\times$  2) of the dried collapsed capsules changed from 71.2 to 139.8 nm.

## RESULTS AND DISCUSSION

**UV-Induced Capsule Shrinkage.**  $(\text{PAH/PMA-BP})_4$  capsule suspensions were exposed to the UV light under a power of 5 mW/cm<sup>2</sup> for different irradiation durations. As shown in

Figure 1, the size change of the capsules is obvious. Before the irradiation, the capsules show round and flat morphologies on the silicon wafer with an average diameter of 5.12 μm (Figure 1a). After being placed under the UV light, the capsule



Scheme 2. Schematic Representation of Cross-Linking Reaction in the Capsule Shells<sup>a</sup>

<sup>a</sup>The photo-cross-linking does not influence the electrostatic interactions between polyanion and polycation.

shrinkage happened immediately. For only 15 min, the average diameter was decreased to  $4.54\ \mu\text{m}$  (Figure 1b). With the increase of UV irradiation time, the capsule size continued to decrease. After 120 min UV irradiation, a significant reduction in the capsule diameter could be found, i.e., the capsule size was reduced to  $3.65\ \mu\text{m}$  (i.e., a reduction of  $\sim 30\%$  in diameter) (Figure 1f). Further increasing the UV irradiation period to 3 h did not show an obvious size decrease. With shrinkage of the capsule, the capsule shell appeared thicker and stronger, which resulted in a three-dimensional spherical capsule appearance under the SEM observation (Figure 1f). The change in capsule diameter and shell thickness could be verified by the AFM results, as shown in Figure 2 (and TEM results in SI Figure S2). After 2 h UV irradiation, the  $(\text{PAH}/\text{PMA-BP})_4$  capsule shell thickness was almost doubled, changed from  $\sim 35\ \text{nm}$  to  $\sim 70\ \text{nm}$ . Furthermore, the irradiated capsules shrank to diameters below  $4\ \mu\text{m}$ , consistent with the SEM results.

In order to investigate the main reason for the shrinkage of  $(\text{PAH}/\text{PMA-BP})_4$  capsules, PAH/PMA-BP multilayer films were made as previously described, and UV-Vis spectroscopy was used to detect the possible UV absorbance change in the films. As shown in SI Figure S3, for the polyelectrolytes used in the experiment, PMA-BP showed a UV absorbance peak at 265 nm wavelength, which could be attributed to the  $\pi-\pi^*$  transition of the benzophenone groups in the polymer chains, totally different from those of PAH, PSS, and PMA. When the electrostatic reaction happened between PAH and PMA-BP polymers, the absorbance peak changed slightly, shifting to 275 nm, as shown in SI Figure S4. With the increase of the number of PAH/PMA-BP layers (i.e., from 8 layers to 64 layers), the absorbance peak became more pronounced, which indicated that there was increasing amount of BP groups deposited on the substrate.

When the multilayer films were exposed to UV light, the absorbance intensity at 275 nm decreased with the irradiation duration, as illustrated in SI Figure S5, which shows the UV-Vis spectra of 64 multilayers of PAH/PMA-BP film on a quartz slide as a function of UV irradiation time. Under UV irradiation, benzophenone groups were excited, and tended to absorb photons from the nearby unreactive C-H bonds, leading to the generation of a new C-C bond and cross-linking within the multilayers.<sup>10</sup> Fourier transform infrared (FTIR) spectra analysis of 0–2 h irradiated  $(\text{PAH}/\text{PMA-BP})_4$  capsules confirmed this chemical transition (see Scheme 2). As shown in Figure 4, the FTIR spectra of the samples containing the BP groups exhibited a decrease in the C=O carbonyl group peak at  $1603\ \text{cm}^{-1}$ , which could be attributed to the deformation of BP radicals after UV irradiation. In addition, the decrease in the aromatic ring at  $1512\ \text{cm}^{-1}$  also verified this BP-related chemical change. However, a broad peak that corresponds to the generation of hydroxyl group (OH) accompanied with BP deformation in the region  $3400\text{--}3500\ \text{cm}^{-1}$  was too weak to be observed.

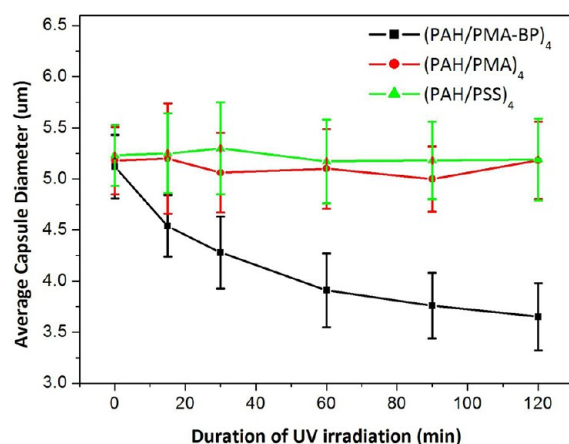


**Figure 3.** Size changes of three different kinds of capsules after UV irradiation. The UV irradiation was fixed at  $5\text{mW}/\text{cm}^2$ . Capsule diameters and distributions were expressed as mean  $\pm$  SD of at least 35 capsules per sample of random measurement of SEM images.

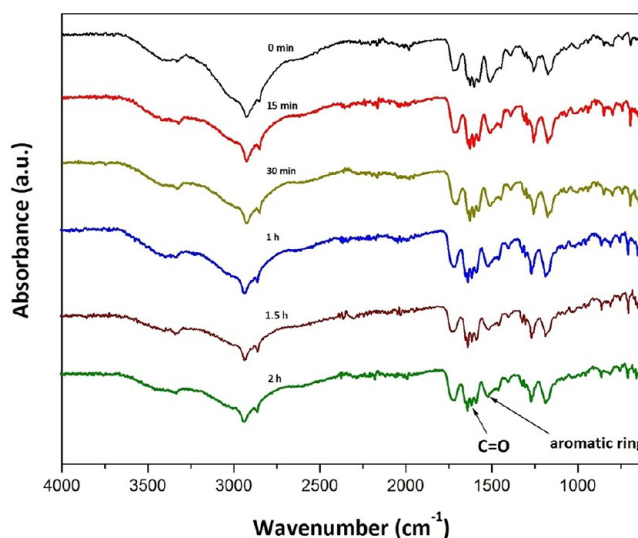


**Figure 4.** FTIR spectra of PAH/PMA-BP samples before (black line) and after (other lines) UV irradiation. The  $1603\ \text{cm}^{-1}$  and  $1512\ \text{cm}^{-1}$  peaks are the benzophenone's carbonyl group (C=O) and aromatic ring skeletal stretch vibrations, respectively.

In the control experiment, other capsules without a BP group such as  $(\text{PAH}/\text{PMA})_4$  and  $(\text{PAH}/\text{PSS})_4$  capsules cannot absorb UV energy at a wavelength between 250 and 600 nm, and exhibit no capsule shrinkage. As shown in Figure 3, capsules with BP groups shrunk from  $5.12 \pm 0.31\ \mu\text{m}$  to  $3.65 \pm 0.33\ \mu\text{m}$  upon 2 h UV irradiation. While the  $(\text{PAH}/\text{PMA})_4$  and  $(\text{PAH}/\text{PSS})_4$  capsules without a BP group showed no obvious shrinkage (SI Figure S6). It has been reported that PSS possesses a maximum UV absorption at  $\sim 220\ \text{nm}$ . Theoret-

ically, exposure of PAH/PSS to UV light will cause a shrinkage in size. As reported by Katagiri,<sup>2b</sup> after 2 h irradiation under a power of 20 mW/cm<sup>2</sup>, PAH/PSS shrunk to less than 50% of their original diameter. However, no obvious PAH/PSS capsule shrinkage could be found in our experiments (Figure 3 and SI Figure S6). The low UV power (only 5 mW/cm<sup>2</sup>) used in our study could be one explanation. Another reason may be the limitation of our UV source. As the UV source is selected predominately to suit the chemical transition of BP groups in this work, a mercury lamp (UVACUBE 100, Honle UV Technology) was used, which only emits a small fraction of UV light at wavelength smaller than 250 nm (i.e., <10%). Consequently, the contribution from the most likely spectral range to have an effect on PSS (i.e., around 220 nm) is small and may well result in no apparent shrinkage of PAH/PSS capsules in our conditions after 2 h irradiation. It should be noted, however, that the PAH/PSS capsules were only used as a control to contrast the BP-related capsule change.

**Capsule Permeability and Stability.** Besides the environmental influencing factors (e.g., pH, ionic strength), the permeability of capsules mainly depends on their shell density. There are different mechanisms of permeability through polyelectrolyte multilayers discussed in the literature involving adsorption in diffusing molecules within multilayers, as well as possible contraction of coils caused by solvent or pH.<sup>14a–d</sup> Generally, the current view is that multilayer densification caused by closely packed polymer segments and hence fewer voids filled with water result in lower probability of molecules to move through.<sup>14a,b</sup> Densification might be the result of polymer rearrangements, as well as cross-linking the chains. Shrinkage is one of the effective methods to increase shell density. Different strategies such as light-induced morphology change<sup>2a</sup> and heat treatment<sup>14a</sup> were used to alter the shell density and influence capsule permeability.<sup>14c</sup> Both, however, suffer from certain limitations: for instance, the former shrinks the capsules through length reduction of the azobenzene molecule caused by trans to cis photoisomerization, while the latter cannot deal with temperature-sensitive materials such as DNA and protein. In contrast to the physical contraction caused by in-plane molecule photoisomerization or heat treatment, benzophenone-related shrinkage requires a stable chemical covalent bonding within multilayers, which leads to a reconfiguration of the neighboring polymer chains, and benefits a new method of engineering steady delivery systems.

In this subexperiment, AF488-labeled dextran (10 kDa) was chosen for the encapsulation study due to its strong fluorescence resistance to photobleaching and, most importantly, good visualization characteristics to demonstrate the changes in permeability of the microcapsules during long periods of irradiation. As shown in Figure 5, confocal laser scanning microscopy (CLSM) images illustrate the dye encapsulation of (PAH/PMA-BP)<sub>4</sub> capsules in the presence of AF488-labeled dextran. Due to the photobleaching, encapsulation can only be viewed after a short irradiation time; consequently, 15 min irradiation result was used as an example here. Before UV irradiation, all the capsules were suspended in the fluorescent polymer solution (the green background) for 1 h, and the fluorescent dextran can permeate into the hollow capsules (Figure 5a). However, due to the porous structure of capsule shells, hollow capsules cannot hold the dye inside (Figure 5b), and only a very small amount of the dye was stuck in the capsule shells. Upon UV irradiation, the capsule shell of the hollow capsules photo-cross-linked, shrank, and

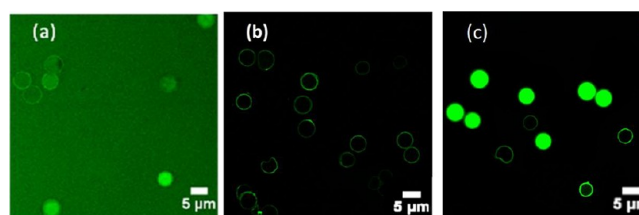


**Figure 5.** CLSM images illustrating the dye encapsulation of (PAH/PMA-BP)<sub>4</sub> capsules in the presence of an AF488-labeled dextran. Before UV irradiation, the fluorescent polymer (green) can permeate into the hollow capsules (a), cannot be held if washed directly (b), but can be encapsulated in the capsules after 15 min irradiation, even after 3 wash steps (c).

closed or reduced the porosity of the shells to keep the dye inside (Figure 5c).

The dye encapsulation limits our study to short irradiation durations due to the photobleaching effect. For longer irradiation periods, we will use the suspensions of already-irradiated capsules to examine the dye penetration effect, which again can demonstrate the capsule permeability changes caused by UV light. As shown in Figure 6 (and SI Figure S7), (PAH/

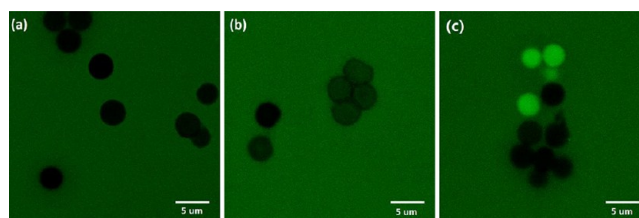


**Figure 6.** CLSM images illustrating the dye permeation of 2-h irradiated (PAH/PMA-BP)<sub>4</sub> capsules in the presence of an AF488-labeled dextran for 0 h (a), 3 h (b), and 4 h (c).

PMA-BP)<sub>4</sub> capsules were first irradiated for 2 h, and were then suspended in AF488-labeled dextran solution. Throughout the dye permeation experiments, aliquots of the sample solutions were taken after a certain incubation time, and then illustrative images were captured to represent typical examples of different dye permeation status (hollow, half-filled, filled). At the beginning, there was no dye permeation into the capsule shells; capsules showed black shadow images under the microscope (Figure 6a). With the increase of time, dye polymers started to penetrate the capsule through the shell network structure or defects. Extending the UV irradiation time to 3 h, it is obvious that the dye polymers had already penetrated into part of the capsules, as the color of the capsules gradually became dark gray (Figure 6b). Four hours later, parts of the capsules were filled with dye polymers. A clear example is presented in Figure 6c, which demonstrates an intermediate state of permeability, i.e., about 40% capsules were filled with dye exhibiting bright green images. Compared with Figure 5a (1 h in dye solution), it is obvious that the UV cross-linking strengthened the capsule shells and decreased the porosity of the shells, resulting in a much stronger shell structure to resist dye penetration.

Fabricating capsules with pH-sensitive weak polyelectrolytes, the charges or ionization degrees along the PAH ( $pK_a = 8.6$ ) and PMA ( $pK_a = 6.8$ ) molecular chains could be controlled by varying the solution pH value. It has been shown that, after LbL assembly,  $pK_a$  values of the electrostatically absorbed PAH-

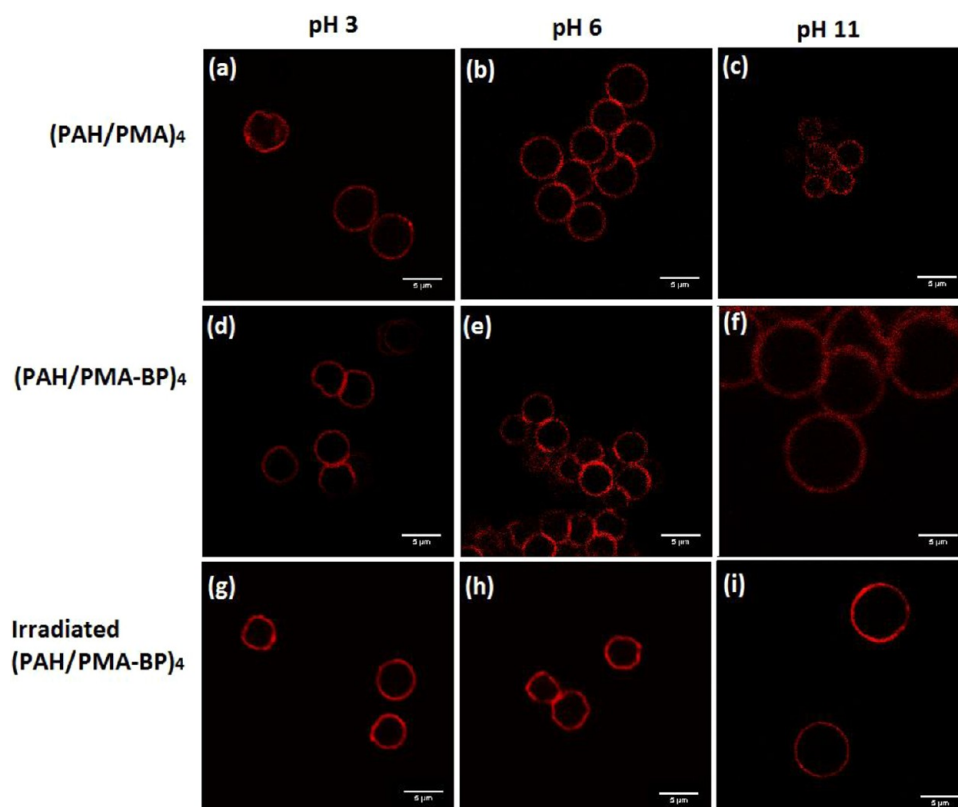


**Figure 7.** CLSM images of different capsules at pH 3, pH 6, and pH 11. (Scale bar: 5  $\mu\text{m}$ ).

PMA multilayers could be shifted by approximately 2–3 pH units to the alkaline ( $\text{p}K_{\text{a}}$ , PAH = 10.8) or acidic ( $\text{p}K_{\text{a}}$ , PMA = 3.9) region, respectively.<sup>17</sup> Therefore, after capsule preparation, electrostatic interactions between the polyanion and the polycation could be influenced by the outer pH environment. Here, we described the pH-dependent behaviors of weak polyelectrolyte microcapsules,  $(\text{PAH}/\text{PMA})_4$  and  $(\text{PAH}/\text{PMA-BP})_4$ , as well as irradiated  $(\text{PAH}/\text{PMA-BP})_4$  capsules.

As shown in Figure 7 (first row), the stability of  $(\text{PAH}/\text{PMA})_4$  capsules in different pH solutions depends on their dissociation behavior, similar to those reported in Mauser's work.<sup>17</sup> At pH = 6, both PAH and PMA are highly charged, and all the capsules were stable with a diameter of  $5.0 \pm 0.30 \mu\text{m}$  (Figure 7b). By decreasing the pH value, PAH was fully charged, but more and more carboxylate ( $-\text{COO}^-$ ) groups of the PMA were deprotonated. At pH = 3 (i.e., below the  $\text{p}K_{\text{a}}$  of PMA in PAH-PMA multilayers), only a small amount of carboxyl ( $-\text{COOH}$ ) groups were dissociated, resulting in PAH with an excess amount of uncompensated ammonium ( $-\text{NH}^{3+}$ ) groups. The electrostatic repulsion between the positive charges of PAH caused a swelling of the shell structure. If the electrostatic repulsion plays a predominant role here, the remaining electrostatic interactions between the minority ionic pairs of PAH and PMA would not be strong enough to stabilize the shell structure. However, at pH = 3, uncharged PMA molecules provided a hydrophobic association, which helped the capsule shell survive and exhibited only a slight size increase to  $5.35 \pm 0.29 \mu\text{m}$  diameter (Figure 7a). Likewise, PMA became fully charged at pH = 11, while most of the PAH got deprotonated. Without a hydrophobic interaction, electrostatic repulsion of the negative charges became the dominant interaction, resulting in the dissolution of the shell (Figure 7c). Adjusting the capsule suspension pH value to 12, capsule

dissolution occurred immediately; no image could be captured. As for the  $(\text{PAH}/\text{PMA-BP})_4$  capsules (second row), the stability of the capsule system composed of PMA-BP is a slightly different. Due to the existence of  $\sim 50\%$  esterified PMA segment, the total amount of PAH in PAH/PMA-BP capsules was only half of that in PAH/PMA capsules in order to obey the rule of charge balance. Thus, an increase in pH led to a more pronounced effect on the PAH/PMA-BP system (Figure 7, second row), exhibiting an early swelling state of capsules at pH = 11. At high pH, the excess amount of uncompensated carboxylate groups of the PMA segment would cause the dissolution of the shell, but the existence of the esterified PMA segment ( $\sim 50\%$  of PMA-BP) played a role in stabilizing the shell structure in basic conditions. As shown in Figure 7f, an immediate dissolution was depressed, resulting in swollen capsules of diameter  $9.71 \pm 0.60 \mu\text{m}$ .

Stabilizing the pH-sensitive multilayers in extreme pH conditions has always been a challenging task. Cross-linking might be an effective method to solve this problem. By cross-linking the functional groups of the individual polyelectrolytes with chemical cross-linkers, good protection is provided against the dissolution of polyelectrolyte multilayers.<sup>18</sup> For instance, if we use a cross-linker, e.g., EDC, to cross-link the functional groups ( $-\text{NH}_2$  and  $-\text{COOH}$ ) of PAH/PMA capsule shells, the multilayer system would become stable in extreme pH conditions. In the meantime, these capsules also become rigid and will not respond to the outer pH anymore, as the charge sites of the multilayers are consumed forming amide bonds ( $-\text{NH}-\text{CO}-$ ). Here, we introduce the photoactive BP groups to cross-link the PAH/PMA capsule. As shown in Scheme 2, UV irradiation causes a recombination of BP and unreactive C–H bond,<sup>19</sup> providing cross-linking sites within multilayers. Unlike the amidation reaction of  $-\text{COOH}$  and  $-\text{NH}_2$  groups,



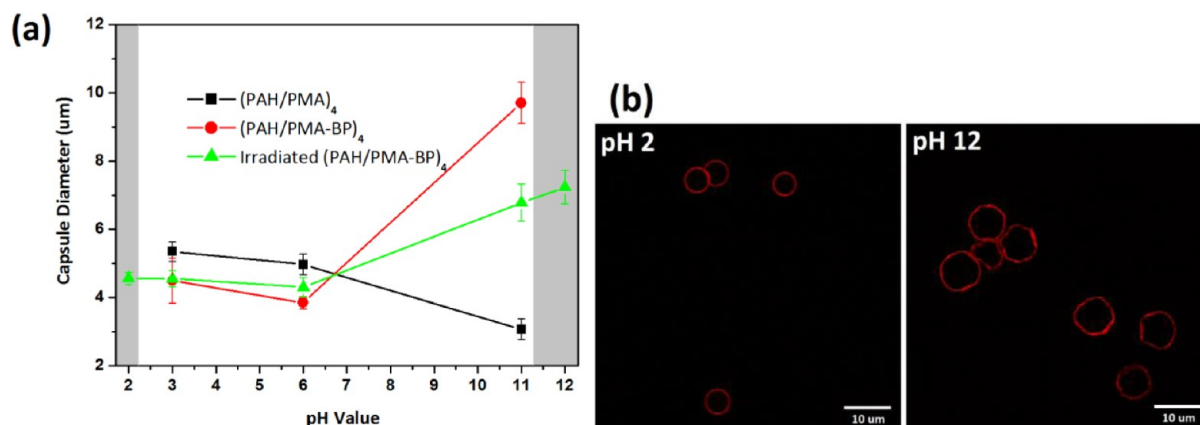


**Figure 8.** Diameter of microcapsules as a function of pH (a) and CLSM images of (PAH/PMA-BP)<sub>4</sub> at pH 2 and pH 12 (scale bar: 10 μm) (b). The gray areas indicate the regions where the non-irradiated capsules are dissolved.

UV cross-linking not only stabilizes the capsules, but also maintains ionizable groups. As shown in Figure 7 (the third row), at pH = 6, capsules irradiated for 15 min are stable with a size of  $4.30 \pm 0.29 \mu\text{m}$  (Figure 7g), which is consistent with the SEM results. By decreasing the pH value, capsules swell slightly and the size is increased to  $4.55 \pm 0.24 \mu\text{m}$  (Figure 7h). Increasing the pH value to 11 increases the capsule size to  $6.79 \pm 0.54 \mu\text{m}$  (Figure 7i). In comparison with the non-irradiated (PAH/PMA-BP)<sub>4</sub> capsules, the UV-cross-linked capsules still possess pH-responsive properties, but not as extreme as the non-irradiated ones. Besides the relatively normal pH range from 3 to 11, capsules in extreme pH conditions are investigated, as shown in Figure 8. After adjusting the capsule suspension to a pH value beyond the  $\text{pK}_a$  values of the PAH/PMA multilayers, a capsule without irradiation cannot survive due to the lack of electrostatic interactions (Figure 8a). However, the UV-irradiated capsules are still stable after suspending in a solution of pH = 2 for 1 week. In comparison with the capsules in a pH = 3 solution, there is no obvious size change of the irradiated (PAH/PMA-BP)<sub>4</sub> capsules at pH = 2, i.e., an average diameter of  $4.56 \mu\text{m}$  is found. However, at pH = 12, the irradiated capsules continue to swell to a diameter of  $7.24 \mu\text{m}$ .

We expect that these (PAH/PMA-BP)<sub>4</sub> microcapsules with UV-responsive properties and pH-dependent stability could provide a novel way to control drug delivery systems, in which UV light could be used to encapsulate chemicals and drugs without heating, and the UV-induced shrinkage, as well as the pH-dependent stability, could be used to modulate their release. Most importantly, it is also expected that the idea of the two-channel controllable microcapsule system with the combination of UV- and pH-responsive properties could excite inspiration to design and engineering multifunctional vesicles for drug delivery, as well as other potential applications.

## CONCLUSION

We reported the fabrication and characterization of UV-responsive (PAH/PMA-BP)<sub>4</sub> capsules from two weak polyelectrolytes enabling pH response. The capsule properties are tunable by the exposure to UV light, i.e., the capsules can shrink about 30% in diameter with nearly doubled shell thickness upon 2 h irradiation at a wavelength of 275 nm. Such UV-triggered shrinkage modified the capsule permeability, providing a novel method for the entrapment of biologically active compound avoiding heating. In addition, (PAH/PMA-BP)<sub>4</sub>

capsules exhibited tunable pH-responsive properties. It is demonstrated that the capsule size and stability can be controlled reversibly by varying the solution pH values. It is shown that, after UV irradiation, cross-linking happened in the capsule shells, increasing the capsule stability in extreme pH conditions. The increased stability did not consume the functional groups of weak polyelectrolytes, which maintained the capsule's pH-responsive capability. These (PAH/PMA-BP)<sub>4</sub> microcapsules with UV-responsive properties and pH-dependent stability could provide a promising approach for drug delivery systems.

## ASSOCIATED CONTENT

### Supporting Information

Additional figures as described. This material is available free of charge via the Internet at <http://pubs.acs.org>.

## AUTHOR INFORMATION

### Corresponding Author

\*Tel: +44-20-7882-5508. Fax: +44-20-7882-3390. E-mail: [g.sukhorukov@qmul.ac.uk](mailto:g.sukhorukov@qmul.ac.uk).

### Notes

The authors declare no competing financial interest.

## ACKNOWLEDGMENTS

We thank Dr. Zofia Luklinska of Nanovision (QMUL) for her help with SEM and TEM measurements.

## REFERENCES

- (1) (a) Meng, F.; Zhong, Z.; Feijen, J. Stimuli-responsive polymersomes for programmed drug delivery. *Biomacromolecules* **2009**, *10* (2), 197–209. (b) Li, M. H.; Keller, P. Stimuli-responsive polymer vesicles. *Soft Matter* **2009**, *5* (5), 927–937. (c) Delcea, M.; Möhwald, H.; Skirtach, A. G. Stimuli-responsive LbL capsules and nanoshells for drug delivery. *Adv. Drug Delivery Rev.* **2011**, *63*, 730–747.
- (2) (a) Bédard, M.; Skirtach, A. G.; Sukhorukov, G. B. Optically driven encapsulation using novel polymeric hollow shells containing an azobenzene polymer. *Macromol. Rapid Commun.* **2007**, *28* (15), 1517–1521. (b) Katagiri, K.; Matsuda, A.; Caruso, F. Effect of UV-Irradiation on Polyelectrolyte Multilayered Films and Hollow Capsules Prepared by Layer-by-layer Assembly. *Macromolecules* **2006**, *39* (23), 8067–8074. (c) Zhu, H.; McShane, M. J. Macromolecule Encapsulation in Diazoresin-Based Hollow Polyelectrolyte Microcapsules. *Langmuir* **2005**, *21* (1), 424–430.

- (3) Yuan, X.; Fischer, K.; Schärfl, W. Photocleavable microcapsules built from photoreactive nanospheres. *Langmuir* **2005**, *21* (20), 9374–9380.
- (4) Bédard, M. F.; Braun, D.; Sukhorukov, G. B.; Skirtach, A. G. Toward self-assembly of nanoparticles on polymeric microshells: near-IR release and permeability. *ACS Nano* **2008**, *2* (9), 1807–1816.
- (5) Skirtach, A. G.; Antipov, A. A.; Shchukin, D. G.; Sukhorukov, G. B. Remote activation of capsules containing Ag nanoparticles and IR dye by laser light. *Langmuir* **2004**, *20* (17), 6988–6992.
- (6) Katagiri, K.; Imai, Y.; Koumoto, K.; Kaiden, T.; Kono, K.; Aoshima, S. Magneto-responsive On-Demand Release of Hybrid Liposomes Formed from Fe<sub>3</sub>O<sub>4</sub> Nanoparticles and Thermosensitive Block Copolymers. *Small* **2011**, *7* (12), 1683–1689.
- (7) Johnston, A. P. R.; Cortez, C.; Angelatos, A. S.; Caruso, F. Layer-by-layer engineered capsules and their applications. *Curr. Opin. Colloid Interface Sci.* **2006**, *11* (4), 203–209.
- (8) (a) Sukhorukov, G. B.; Donath, E.; Lichtenfeld, H.; Knippel, E.; Knippel, M.; Budde, A.; Möhwald, H. Layer-by-layer self assembly of polyelectrolytes on colloidal particles. *Colloids Surf., A* **1998**, *137* (1–3), 253–266. (b) Lulevich, V. V.; Andrienko, D.; Vinogradova, O. I. Elasticity of polyelectrolyte multilayer microcapsules. *J. Chem. Phys.* **2004**, *120*, 3822. (c) Nakamura, M.; Katagiri, K.; Koumoto, K. Preparation of hybrid hollow capsules formed with Fe<sub>3</sub>O<sub>4</sub> and polyelectrolytes via the layer-by-layer assembly and the aqueous solution process. *J. Colloid Interface Sci.* **2010**, *341* (1), 64–68. (d) Vinogradova, O. I.; Lebedeva, O. V.; Kim, B. S. Mechanical behaviour and characterization of microcapsules. *Annu. Rev. Mater. Sci.* **2006**, *36*, 143–178.
- (9) (a) Ariga, K.; Lvov, Y. M.; Kawakami, K.; Ji, Q.; Hill, J. P. Layer-by-layer self-assembled shells for drug delivery. *Adv. Drug Delivery Rev.* **2011**, *63* (9), 762–771. (b) Sukhishvili, S. A.; Kharlampieva, E.; Izumrudov, V. Where polyelectrolyte multilayers and polyelectrolyte complexes meet. *Macromolecules* **2006**, *39* (26), 8873–8881. (c) Balkundi, S. S.; Veerabadran, N. G.; Eby, D. M.; Johnson, G. R.; Lvov, Y. M. Encapsulation of Bacterial Spores in Nanoorganized Polyelectrolyte Shells. *Langmuir* **2009**, *25* (24), 14011–14016. (d) Skirtach, A. G.; Yashchenok, A. M.; Möhwald, H. Encapsulation, release and applications of LbL polyelectrolyte multilayer capsules. *Chem. Commun.* **2011**, 47 (48), 12736–12746.
- (10) Dorman, G.; Prestwich, G. D. Benzophenone photophores in biochemistry. *Biochemistry* **1994**, *33* (19), 5661–5673.
- (11) (a) Kim, B. S.; Vinogradova, O. I. pH-controlled swelling of polyelectrolyte multilayer microcapsules. *J. Phys. Chem. B* **2004**, *108* (24), 8161–8165. (b) Kozlovskaya, V.; Sukhishvili, S. A. Amphoteric hydrogel capsules: Multiple encapsulation and release routes. *Macromolecules* **2006**, *39* (18), 6191–6199. (c) Lulevich, V. V.; Vinogradova, O. I. Effect of pH and Salt on the Stiffness of Polyelectrolyte Multilayer Microcapsules. *Langmuir* **2004**, *20* (7), 2874–2878.
- (12) Park, M. K.; Deng, S.; Advincula, R. C. pH-sensitive bipolar ion-permeable ultrathin films. *J. Am. Chem. Soc.* **2004**, *126* (42), 13723–13731.
- (13) Volodkin, D. V.; Petrov, A. I.; Prevot, M.; Sukhorukov, G. B. Matrix polyelectrolyte microcapsules: new system for macromolecule encapsulation. *Langmuir* **2004**, *20* (8), 3398–3406.
- (14) (a) Köhler, K.; Sukhorukov, G. B. Heat treatment of polyelectrolyte multilayer capsules: a versatile method for encapsulation. *Adv. Funct. Mater.* **2007**, *17* (13), 2053–2061. (b) Ibarz, G.; Dähne, L.; Donath, E.; Möhwald, H. Controlled Permeability of Polyelectrolyte Capsules via Defined Annealing. *Chem. Mater.* **2002**, *14* (10), 4059–4062. (c) De Geest, B. G.; Sanders, N. N.; Sukhorukov, G. B.; Demeester, J.; De Smedt, S. C. Release mechanisms for polyelectrolyte capsules. *Chem. Soc. Rev.* **2007**, *4*, 636–649. (d) Kim, B. S.; Lebedeva, O. V.; Koynov, K.; Gong, H.; Glasser, G.; Lieberwith, I.; Vinogradova, O. I. Effect of Organic Solvent on the Permeability and Stiffness of Polyelectrolyte Multilayer Microcapsules. *Macromolecules* **2005**, *38* (12), 5214–5222.
- (15) Mauser, T.; Déjournat, C.; Möhwald, H.; Sukhorukov, G. B. Microcapsules made of weak polyelectrolytes: templating and stimuli-responsive properties. *Langmuir* **2006**, *22* (13), 5888–5893.
- (16) Volodkin, D. V.; Larionova, N. I.; Sukhorukov, G. B. Protein encapsulation via porous CaCO<sub>3</sub> microparticles templating. *Bio-macromolecules* **2004**, *5* (5), 1962–1972.
- (17) Mauser, T.; Déjournat, C.; Sukhorukov, G. B. Reversible pH-Dependent Properties of Multilayer Microcapsules Made of Weak Polyelectrolytes. *Macromol. Rapid Commun.* **2004**, *25* (20), 1781–1785.
- (18) (a) Elsner, N.; Kozlovskaya, V.; Sukhishvili, S. A.; Fery, A. pH-Triggered softening of crosslinked hydrogen-bonded capsules. *Soft Matter* **2006**, *2* (11), 966–972. (b) Tong, W.; Gao, C.; Möhwald, H. Stable Weak Polyelectrolyte Microcapsules with pH-Responsive Permeability. *Macromolecules* **2006**, *39* (1), 335–340.
- (19) Prucker, O.; Naumann, C. A.; Rühle, J.; Knoll, W.; Frank, C. W. Photochemical attachment of polymer films to solid surfaces via monolayers of benzophenone derivatives. *J. Am. Chem. Soc.* **1999**, *121* (38), 8766–8770.